

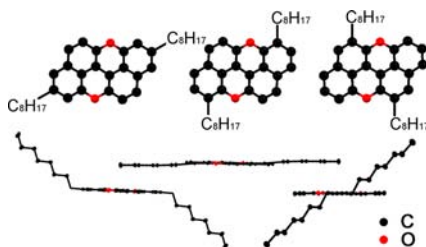
Synthesis, Properties, and Structures of
Functionalized *peri*-XanthenoxantheneNa Lv,^{†,‡,§} Meilan Xie,[†] Weibing Gu,[†] Huanyang Ruan,[†] Song Qiu,^{*,†}
Chunshan Zhou,[†] and Zheng Cui[†]

Printable Electronics Research Centre, Suzhou Institute of Nano-Tech and
Nano-Bionics, CAS, Suzhou, 215123, China, Technical Institute of Physical and
Chemistry, CAS, Beijing, 100190, China, and University of Chinese Academy of
Sciences, CAS, Beijing, 100049, China

sqliu2010@sinano.ac.cn

Received March 25, 2013

ABSTRACT



Three types of alkylated *peri*-xanthenoxanthene (PXX) have been synthesized employing efficient synthetic routes. These heteroaromatic compounds exhibited different electronic and crystal structures according to UV–vis spectra, electrochemical measurements, and X-ray structural analyses. Among them, 1,7-DOPXX has been demonstrated as an active material for organic field-effect transistors with promising mobility and a high on/off ratio simultaneously.

The design and synthesis of polycyclic aromatic compounds are of great interest owing to their potential applications as organic semiconductors for electronic devices, such as organic field-effect transistors (OFETs),¹ light emitting diodes (LEDs),² and photovoltaic cells.³ In particular, heteroaromatic containing chalcogenophenes

(thiophene or selenophene) in fused aromatic ring systems has been actively investigated because of their remarkable electronic properties for OFETs.⁴ However, most of heteroaromatic compounds containing chalcogen are pentacyclic instead of hexacyclic. From the synthetic chemistry viewpoint, efficient synthetic strategies for conjugated hexacyclic heteroaromatic compounds containing chalcogen are limited.

peri-Xanthenoxanthene (PXX), which is a less reported conjugated hexacyclic aromatic compound containing chalcogen, has been employed as pigments⁵ and as the species of charge transfer complexes.⁶ Recently, PXX and its derivatives have been investigated by Merck and Sony as organic semiconductors due to their excellent carrier transport capacity and good environmental stability.⁷

To synthesize PXX, Tamotsu et al. used Cu(OAc)₂ to oxidize the alkaline solution of 1,1'-bi-2-naphthol,⁸ and

[†] Printable Electronics Research Centre, Suzhou Institute of Nano-Tech and Nano-Bionics, Chinese Academy of Sciences.

[‡] Technical Institute of Physical and Chemistry, Chinese Academy of Sciences.

[§] University of Chinese Academy of Sciences.

(1) (a) Wang, C.; Dong, H.; Hu, W.; Liu, Y.; Zhu, D. *Chem. Rev.* **2012**, *112*, 2208–67. (b) Beaujuge, P. M.; Fréchet, J. M. J. *J. Am. Chem. Soc.* **2011**, *133*, 20009–20029. (c) Takimiya, K.; Shinamura, S.; Osaka, I.; Miyazaki, E. *Adv. Mater.* **2011**, *23*, 4347–4370. (d) Dong, H.; Wang, C.; Hu, W. *Chem. Commun. (Camb)* **2010**, *46*, 5211–22.

(2) (a) Tao, Y.; Yang, C.; Qin, J. *Chem. Soc. Rev.* **2011**, *40*, 2943–2970. (b) Xiao, L.; Chen, Z.; Qu, B.; Luo, J.; Kong, S.; Gong, Q.; Kido, J. *Adv. Mater.* **2011**, *23*, 926–952.

(3) Liu, J.; Walker, B.; Tamayo, A.; Zhang, Y.; Nguyen, T.-Q. *Adv. Funct. Mater.* **2013**, *23*, 47–56.

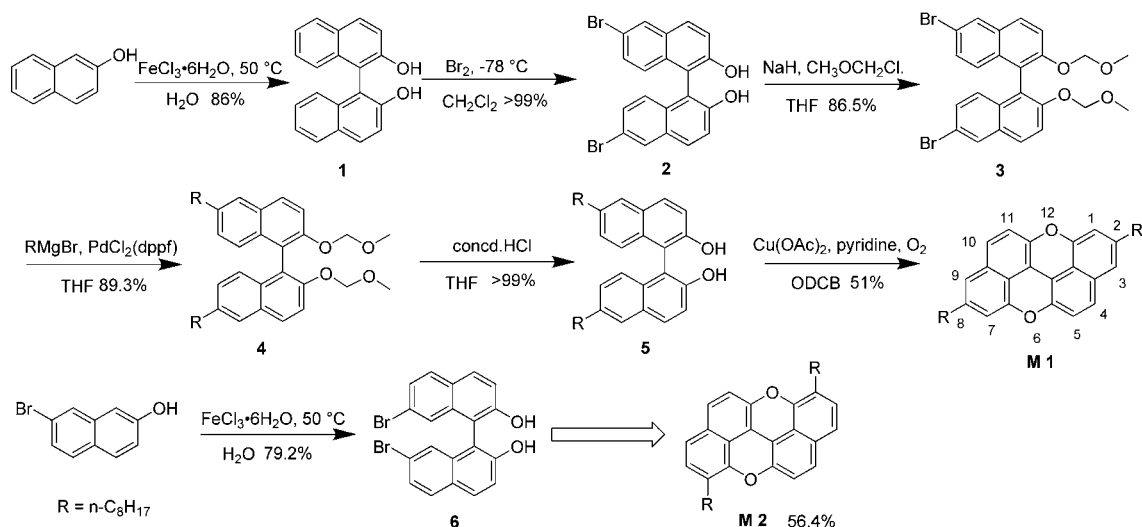
(4) (a) Yamamoto, T.; Nishimura, T.; Mori, T.; Miyazaki, E.; Osaka, I.; Takimiya, K. *Org. Lett.* **2012**, *14*, 4914–4917. (b) Takimiya, K.; Shinamura, S.; Osaka, I.; Miyazaki, E. *Heterocycles* **2011**, *83*, 1187–1204. (c) Gao, P.; Beckmann, D.; Tsao, H. N.; Feng, X.; Enkelmann, V.; Baumgarten, M.; Pisula, W.; Müllen, K. *Adv. Mater.* **2009**, *21*, 213–216. (d) Nakano, M.; Mori, H.; Shinamura, S.; Takimiya, K. *Chem. Mater.* **2011**, *24*, 190–198.

(5) Prowse, W. G.; Arnot, K. I.; Recka, J. A.; Thomson, R. H.; Maxwell, J. R. *Tetrahedron* **1991**, *47*, 1095–1108.

(6) Asari, T.; Kobayashi, N.; Naito, T.; Inabe, T. *Bull. Chem. Soc. Jpn.* **2001**, *74*, 53–58.

(7) Kobayashi, N.; Sasaki, M.; Nomoto, K. *Chem. Mater.* **2009**, *21*, 552–556.

Scheme 1. Synthetic Route to 2,8-Substituted PXX (**M1**) and 1,7-Substituted PXX (**M2**)



Philipp et al. used transition metal oxide (MnO_2 , CuO , etc.) to oxidize 1,1'-bi-2-naphthol at elevated temperatures.⁹ However, the isolated raw product had to undergo repetitive sublimation to obtain pure PXX. The subsequent functionalization was centered on the para-position of oxygen atoms to give 3,9-substituted PXX, since it is the most active site. However, due to the poor solubility of PXX and Br-PXX, further modification is difficult and may introduce impurity.

Here we report a simple and efficient method to synthesize substituted PXXs. To overcome the purification difficulty, the precursor was functionalized before ring closure. 1,1'-Bi-2-naphthol (**1**) was prepared by a two-phase oxidative coupling of 2-naphthol suspended in aqueous Fe^{3+} solution.¹⁰ With direct bromination followed by a hydroxy-protection reaction with sodium hydride and chloromethyl methyl ether to obtain 6,6'-dibromo-2,2'-bis(methoxymethoxy)-1,1'-binaphthyl (**3**), we can realize the functionalization at the 6,6'-position through existing coupling methods (i.e., Kumada, Suzuki, Stille coupling, etc.). The importance of alkyl substituents has been studied thoroughly, as it can improve solubility and impact the packing of molecules through noncovalent-induced ordering.¹¹ The same principle was applied to alkyl-substituted PXX, i.e. $\text{R} = n\text{-C}_8\text{H}_{17}$. The subsequent deprotection with conc. HCl and microwave assisted cyclization reaction in the presence of $\text{Cu}(\text{OAc})_2$ in O-dichlorobenzene at 220°C yielded desirable 2,8-dioctyl-*peri*-xanthenoxanthene (**M1**, 2,8-DOPXX).

Similarly, starting from 7-bromo-2-naphthol and using the same synthetic procedure as mentioned above, we obtained 1,7-dioctyl-*peri*-xanthenoxanthene (**M2**, 1,7-DOPXX) in a yield of 56.4% (Scheme 1).

When the hydroxy groups of 1,1'-bi-2-naphthol were protected first, selective bromination at the ortho-position of the hydroxy group could be achieved via lithiation of 2,2'-bis(methoxymethoxy)-1,1'-binaphthyl (**7**) followed by trapping with dibromotetrachloroethane, and then the functionalization of (**7**) at the 3,3'-position could be realized through many common coupling methods. However, when it comes to alkylation, using bromoalkane with the assistance of butyllithium to yield 3,3'-dioctyl-2,2'-bis(methoxymethoxy)-1,1'-binaphthyl (**9**) proved to be more simple and direct compared to Kumada coupling. The subsequent deprotection and cyclization reaction yielded 5,11-dioctyl-*peri*-xanthenoxanthene (**M3**, 5,11-DOPXX) (Scheme 2).

The intermediates and products were characterized by ^1H NMR, ^{13}C NMR, and mass spectrometry; the X-ray crystal structures for three alkylated PXXs were also obtained. To the best of our knowledge, crystal structures of substituted PXXs at these positions have never been reported previously.

Figure 1 shows the UV-vis absorption spectra and mirror-plane symmetrical emission spectra of the three compounds. All of them show well-resolved vibrational energy bands, which can be interpreted as a consequence of a highly rigid, planar π -system in these PXX derivatives. Energy gaps estimated from absorption edges are 2.69, 2.68, and 2.72 eV for **M1**, **M2**, and **M3**, respectively. Examination of Figure 1 reveals that the absorption spectra of **M3** are blue-shifted compared with **M1** and **M2**. We assume that the alkyl position may influence the delocalization of electrons on the fused aromatic ring.¹²

(8) Asari, T.; Kobayashi, N.; Naito, T.; Inabe, T. *Bulletin of the Chemical Society of Japan* **2001**, *74*, 53–58.

(9) Stoessel, P.; Buesing, A.; Heil, H. U.S. Patent No. US 2010/0013381 A1.

(10) Ding, K.; Yang, W.; Zhang, L.; Yangjie, W.; Matsuura, T. *Tetrahedron* **1996**, *52*, 1005–1010.

(11) Curiel, D.; Más-Montora, M.; Uruvakili, A.; Orenes, R. A.; Pallamreddy, H.; Molina, P. *Org. Lett.* **2010**, *12*, 3164–3167.

(12) Wang, L.; Duan, G.; Ji, Y.; Zhang, H. *J. Phys. Chem. C* **2012**, *116*, 22679–22686.

Scheme 2. Synthetic Route to 5,11-Substituted PXX (**M3**)

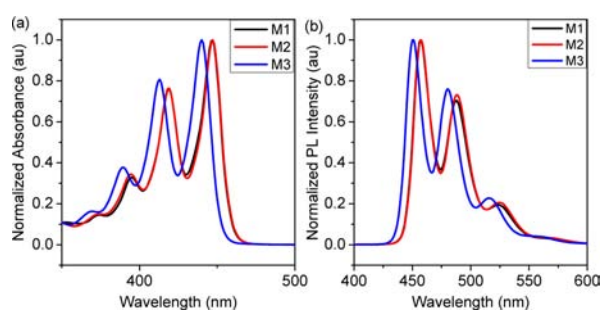
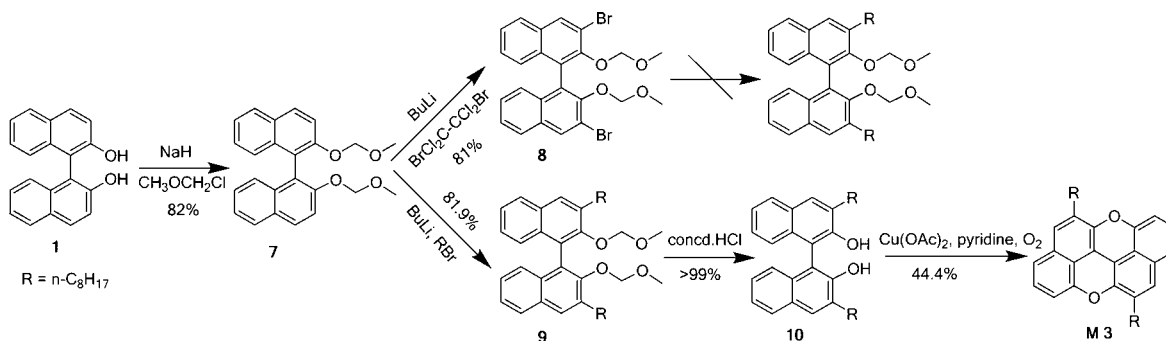


Figure 1. (a) Normalized absorption and (b) emission spectra of **M1–M3**.

Electrochemical characterization was carried out by cyclic voltammetry in dichloromethane solution (Figure S1). All compounds exhibit two reversible or quasi-reversible one-electron oxidation peaks within the span of the electrolyte window, which demonstrate the good electrical stability of the PXX's radical cation. The HOMO energy level estimated from the oxidation onset are ca. -5.06 , -4.92 , and -5.02 eV for **M1**, **M2**, and **M3**, respectively, matching well with the work function of gold. The optical and electrochemical characterization are summarized in Table 1.

Table 1. Optical, Electrochemical Characterization and OFET Properties of **M1–M3**

| compd | E_g^{opt} (eV) ^a | E_{HOMO} (eV) ^b | E_{LUMO} (eV) ^c | μ (cm ² /V·s) ^d | $I_{\text{on}}/I_{\text{off}}$ |
|-----------|---|--|--|--|--------------------------------|
| M1 | 2.69 | -5.01 | -2.32 | 0.04 | 2.6×10^7 |
| M2 | 2.68 | -4.92 | -2.24 | 0.5 | 3.9×10^6 |
| M3 | 2.72 | -5.02 | -2.30 | 0.32 | 1×10^5 |

^a Recorded in dichloromethane (10^{-5} M) at room temperature and estimated from the absorption edge of the solution. ^b Electrochemically determined vs Fc/Fc⁺ in CH₂Cl₂ (10^{-3} M) at room temperature, TBAPF₆ (0.1 M), scan speed 0.1 V/s, SCE reference electrode, Pt working electrode and calculated according to $E_{\text{HOMO}} = -(E_{\text{ox}}^{1/2} + 4.80)$. ^c Values calculated according to $E_{\text{LUMO}} = E_g^{\text{opt}} + E_{\text{HOMO}}$. ^d Estimated from the saturation regime.

Single crystals of **M1–M3** were grown by slow diffusion of ethanol into their tetrahydrofuran solution. Figure S2 shows the bond lengths of the three compounds from X-ray analyses. The decreased bond equalization in **M3**, i.e. the bond length of C=C bond adjacent to the C—O bond, is equal to 1.379 Å for **M1** and 1.382 Å for **M2**, while it is much shorter (1.361 Å) in **M3**, revealing that the PXX unit is less delocalized in **M3** than in **M1** and **M2**, which may explain the blue shift of **M3** in the UV–vis absorption and fluorescence spectra.

The crystal packing of three compounds are compared in Figure 2 (alkyl is omitted for clarity). **M1** and **M3** both display a herringbone packing motif with the π -stacking of the molecules extending along the *b*-axis. **M1** adopts a sandwiched herringbone structure in which the interplanar packing distance is 3.40 Å, and the shortest intermolecular distance (C—H...C between two neighboring cores) is

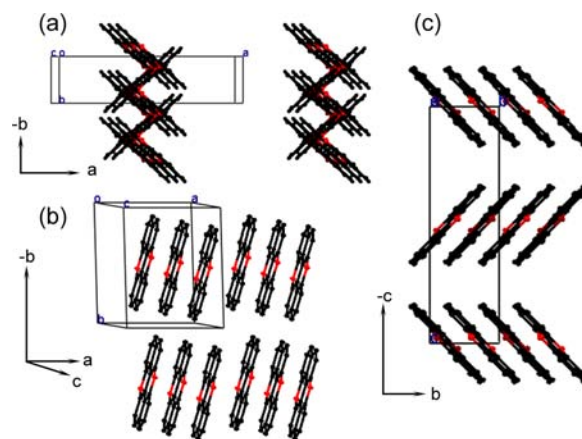


Figure 2. Crystal structures of **M1** (a), **M2** (b), and **M3** (c).

2.54 Å. However, **M3** packs in the conventional herringbone motif in which its dimers are packed in an end-to-face manner with the interplanar packing distance similar to that of **M1** (3.35 Å), but the shortest intermolecular distance is longer (2.79 Å). In contrast, **M2** adopts a fairly

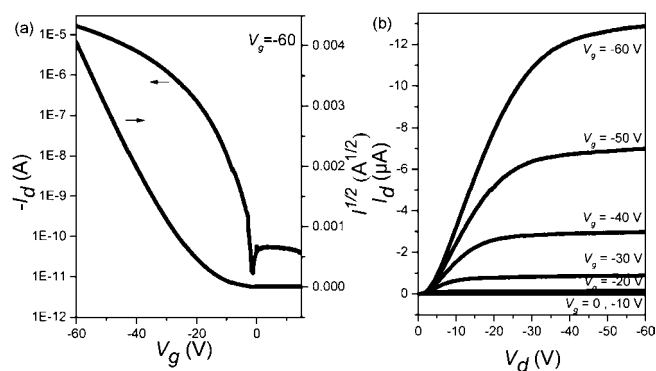


Figure 3. FET characteristics of **M2**: (a) transfer plots and (b) output plots. (For **M1** and **M3**, see Supporting Information.)

flat molecular structure without disturbance of the alkyl, which leads to a one-dimensional slipped face-to-face arrangement with a large slippage of molecules. The molecular stacking distance along the *b*-axis is only 2.83 Å. Meanwhile alkyl chains can interact with the aromatic system through C–H... π contact (2.34 Å) and further stabilize the packing, which is favorable for charge carrier transport.

The thermal stability of the three compounds was evaluated by thermogravimetric analysis (TGA) (Figure S3). The data reveal that they all have good thermal stability with none of them showing significant mass loss up to 312, 296, and 285 °C for **M1**, **M2**, and **M3** respectively (corresponding to a 2% loss of weight).

Transistors with bottom contact and bottom gate geometry were fabricated to investigate the charge transport properties of the synthesized PXX derivatives. The gold source–drain electrodes were prepared by photolithography and were treated with pentafluorothiophenol before

spin coating a 3 mg/mL solution of DOPXX in chlorobenzene, and the subsequent chloroform vapor annealing¹³ would facilitate the formation of large area crystals.

The XRD patterns of thin films are shown in Figure S4. The high crystallinity of **M3** may contribute to the higher mobility compared with **M1**; in fact, **M1** tends to form dendritic and discontinuous crystals other than large plate-like crystals using the spin coating method. The preliminary results show the mobilities for **M1**, **M2**, and **M3** to be 0.04–0.5 cm²·V^{−1}·s^{−1} in the saturation regime with an on/off ratio of 10⁵–10⁷ (Figure 3, Figure S5). Further experiments to optimize device fabrication, particularly molecular arrangement in the thin-film state, are underway, and results will be reported in due course.

In summary, we have developed a simple and efficient synthetic route for the preparation of *peri*-xanthene-anthene (PXX) derivatives with an alkyl in different substituent positions. This synthetic approach offers the opportunity to prepare a new class of functionalized conjugated heteroaromatic compounds containing chalcogen, which show promising hole-transporting ability and good stability. Furthermore, the different substitution positions can influence the solid state packing mode of the molecule to a large extent and has a strong influence on the charge transporting property.

Acknowledgment. This work was supported by Natural Science Foundation of China (91123034, 21104091), the Knowledge Innovation Programme of the Chinese Academy of Sciences (KJCX2-EW-M02).

Supporting Information Available. Synthetic details, characterizations data, TGA, electrochemical studies, OTFTs performance, and crystallographic information files (CIF) for 2,8-DOPXX (**M1**), 1,7-DOPXX (**M2**), and 5,11-DOPXX (**M3**). This material is available free of charge via the Internet at <http://pubs.acs.org>.

(13) Liu, C.; Li, Y.; Xu, Y.; Minari, T.; Li, S.; Takimiya, K.; Tsukagoshi, K. *Org. Electron.* **2012**, *13*, 2975–2984.

The authors declare no competing financial interest.